International Journal of Multiphysics
Volume 18, No. 2, 2024
ISSN: 1750-9548

Optimization of High-Rise Building Retrofitting Against Wind Loads

Mohamed Abdel-Hamed[a*], Rania Samir[b], Atef Eraky[c] , and Abdallah Salama[d]

[a] Lecturer Assist. at Structural Engineering Dept, Faculty of Engineering, Zagazig University, Zagazig, Egypt.
* Corresponding Author. E-Mail: ma.ata@eng.zu.edu.eg
[b] Professor at Structural Engineering Dept, Faculty of Engineering, Zagazig University, Zagazig, Egypt.
E-Mail: rmamien@eng.zu.edu.eg
[c] Professor of at Structural Engineering Dept, Faculty of Engineering, Zagazig University, Zagazig, Egypt.
E-Mail: aeamien@eng.zu.edu.eg
[d] Lecturer at Structural Engineering Dept, Faculty of Engineering, Zagazig University, Zagazig, Egypt.
E-Mail: asabdullatif@eng.zu.edu.eg

Abstract

As the height of any structure increases, it becomes slenderer and more sensitive to wind loads. So, any increase in the structure height that was not considered during the initial stages of the design process will cause many structural issues. For such a problem, structural retrofitting is suggested to resist wind loads and satisfy safety and serviceability requirements. The strategy of retrofitting includes adding structural steel wind-resisting systems in the openings of the structural plan. This paper proposes an optimization technique for steel systems used to retrofit high-rise buildings, which aims to reduce the weight of the steel system keeping the building meeting the constraints of lateral displacement at the top of the building using Genetic Algorithm (GA) as an optimization algorithm. Integrated with CSI ETABS, the Visual Basic application is designed to perform this task. The proposed technique is applied to two cases of reinforced concrete buildings that are vulnerable to wind loads. The first case depicts a sense of consistency within buildings, while the second case exemplifies instances of irregularity in architectural design. Both cases are studied at heights of 15, 18, 21, 24, and 27 stories. The results show that strengthening a building using the optimized steel-braced frame is an efficient technique. The stiffness distribution of the optimum retrofitting system is concluded and formulas describing this distribution are derived.

Keywords: High-rise building, Optimization, Wind loads, Retrofitting, Genetic algorithm

1. Introduction

Super-tall buildings have grown increasingly taller and more flexible due to technological improvements in construction and the development of lightweight, high-strength materials, which have boosted elastic and aerodynamic effects[1], [2]. In recent decades, the popularity of vertical cities with tall buildings has recently increased around the world[3]. As the structure's height increases, more challenges face engineers, as the structure's height is directly proportional to the intensity of lateral loads, such as wind and earthquake[4].

The impact of wind loads on structural safety and comfort design is becoming more and more evident, particularly in complex wind fields[5]. Three general types of wind-induced vibration of super-tall buildings can be distinguished: torsional, along-wind, and across-wind[6]–[8]. When a building is exposed to strong, regular winds that blow perpendicular to its major axis, lateral forces can trigger the structure to sway from one side to the other. This phenomenon is commonly referred to as across-wind vibration[9]. Along-wind vibration occurs

when a building undergoes lateral oscillations parallel to the direction of the prevailing wind, which can be correlated with the wind hitting[10]. The third type of wind-induced vibration is associated with non-uniform wind load distribution resulting in twisting torque along the vertical axis of the building, which causes torsional vibration[11]. To face such kinds of wind-induced vibrations on a laterally weak-resistant tall building, structural retrofitting can be a proposed solution. Structural retrofitting of an existing building that is vulnerable to wind loads has always been an issue of how to balance safety, serviceability, and economy[12]. The economy is the factor that takes the most concern during structural retrofitting, where the system, which will be used as an optimal strengthening system to the building against wind loads, has the minimum cost and meets the requirements of safety and serviceability. Steel structure systems are always used in high-rise buildings, as steel has many advantages, such as a high strength-to-weight ratio, variety of available strength values, and greater variety of sections as well it's easy to assemble and install in the field[4].

There are many techniques to strengthen a building against wind loads, such as columns jacketing with steel, carbon fiber reinforced polymers (CFRPs), or glass fiber reinforced polymers (GFRPs). The installation of auxiliary dampers in tall buildings can be used as a useful solution that has proved its efficiency in controlling the vibrations induced by wind. However, the tall building owners will be highly charged by the massive costs of construction, operation, and maintenance of these solutions, which are high to be afforded [13]–[15]. Miano et al.[16] compared FRP, RC jacketing, and shear walls based on the performance assessment of bare frames. Karihoo et al.[17] studied the retrofitting using a technique based on compatible material with concrete called CARDIFRCs and illustrated that the technique overcomes the mismatching problem of FRP related to mismatching of the tensile strength and stiffness with the retrofitted concrete. They also indicated that CARDIFRCs are a suitable retrofitting technique since they increase the durability of existing RC structures. Rafiqul et al.[18] designed some retrofitting alternatives on an existing RC structure and ranked them using various criteria. Steel bracing was found as the best retrofit technique over steel jacketing, GFRP wrapping, and concrete jackets. Kim et al.[19] compared three bracing systems to diagonal, Chevron, and X-shaped to obtain the most effective system to enhance the performance of tall buildings against seismic and wind loads and found that the Chevron brace shows the best performance over the other two systems by approximately 60 % for wind resistance. Vafai et al.[20] studied the feasibility of using single diagonal bracing for improvement of the lateral response of tall buildings and obtained that the simple diagonal bracings are suitable for typical building frames compared with traditional X-braced frameworks as it reduces the lateral deflection of the typical 24-story building by approximately 2 %. When outriggers (ORs)/ ORs and belt-trusses (BTs) are specially added in tall buildings, the maximum lateral drift (MLD) and the core base moment (CBM) are reduced by 68% and 71%, respectively[2].

Optimizing the weight of the braced steel frame and obtaining the optimal stiffness distribution for columns and bracings will provide a suitable technique and affordable cost for owners to strengthen their buildings that suffer against wind loads and increase the economic feasibility of their ownership. Most researchers work on the structural optimization of tall buildings against seismic loads in the early design stages[21], [22]. Fewer research efforts have been discussed on the optimization of retrofitting and strengthening the building under wind excitations[12]. Previous optimization research worked on different ways of optimization. Chan et al.[23], [24] developed a series of construction methods to maximize structural wind resistance based on the Optimal Criteria (OC) algorithm while lowering the cost of tall rectangular structures that must adhere to lateral drift and acceleration performance limits brought on by wind excitations. Huang et al.[25] proposed an automated computer-based method that reduces the construction expenditures of high-rise steel structures by combining stiffness optimization techniques with aerodynamic wind tunnel load modeling. Li and Li[26] performed the optimum design of skyscrapers excited by wind and used examples of irregular skyscrapers to verify the efficiency of this method resting on virtual work principles and the Rayleigh quotient. Xu et al.[27] implemented a structurally optimized plan for a skyscraper with a complicated structural framework, taking into account lateral displacement limits. Fu et al.[28] proposed a technique to handle the frequency limitation of high-rise buildings under wind loads. This method used the eigenvalue approach for explicitly formulating the frequency constraints and a quadratic programming method for computing the Lagrangian multipliers in the optimization. Gholizadeh et al.[29] proposed a modified particle swarm optimization algorithm (MPSO) to solve the optimization problem of high-rise buildings compared with standard PSO and other techniques and found that MPSO represents the best

technology and can be used effectively to optimize the design of large steel structures. Chan et al.[30] proposed a hybrid optimization algorithm that combines OC and GA methods and used both to design high-rise concrete building structures. They found that GA shows better performance in the local search of numerical optimization problems. On the other hand, the hybrid OC-GA method requires fewer objective function evaluations, so it can handle large-scale optimization problems. Lu et al.[31] proved the feasibility and effectiveness of a hybrid genetic algorithm (GA) and optimal criteria (OC) method for the optimization of high-rise buildings.

This paper proposes an optimal retrofitting technique for structural wind-resisting systems that are used to structurally enhance tall buildings, using Genetic Algorithm (GA) as an optimization algorithm, which aims to minimize the weight of the steel wind-resisting system while meeting the constraints of top lateral displacement and inter-story drift ratio. Visual Basic (VB) .Net application integrated with CSI ETABS is designed to handle the optimization process. This application is supported by a Graphical User Interface (GUI) that facilitates its users to perform optimization processes on any tall building. This procedure is applied to two cases of tall buildings; The first case embodies a consistent pattern evident in the architectural plan and elevation. Conversely, the second case highlights an irregularity. In this instance, the structure exhibits dual heights, with one portion elevated to a predetermined level and the remaining half raised to a height 1.5 times that of the former. Both cases are studied at different heights as numerical models. The stiffness distribution of the steel wind-resisting system is concluded in both, and formulas describing this distribution are derived.

2. Methods

2.1 Joint Simulation Using VB And CSI ETABS

During structurally optimized designs, boundary conditions, such as maximum structural stress and displacement, implicitly serve as functions of design variables. Using traditional techniques, design variable constraints are clearly expressed through complex equations that require significant calculation time and computer capacity to execute a finite element analysis program. Furthermore, it is challenging to create a mathematical model that can precisely represent boundary conditions and design variables for huge and complicated structures. The optimization process of the steel-braced frame is summarized as follows. The universal commercial analysis software CSI ETABS2016 is used along with VB to form an optimization procedure. In detail, ETABS runs multiple loop iterations of the case study building models with different sections for both columns and vertical x-shape bracing. These iterations are looped based on the principles of Genetic Algorithm (GA) which are programmed on VB.

The process of joint simulation starts with creating a base model for the case study building on ETABS with random sections for columns and vertical x-shape bracing. Through CSI ETABS API codes that are programmed on VB, the created base model is opened with ETABS, and the sections of columns and bracings are changed based on the GA. After that, ETABS runs the modified model and sends the results to VB. Then the process continues to obtain the optimal stiffness distribution of the steel-braced frame.

2.2 Optimization model

There are two models used in this study. Both models are a 3D rectangular RC building strengthened with a 3D steel braced frame. The retrofitting optimization problem can be stated as follows:

Minimize

$$W_S = W_{DL_2} - W_{DL_1} \quad (1)$$

Subjected to $d_T \leq d_T{}^U$ (2)

$$d_i \leq d_i{}^U \quad (3)$$

Equation (1) defines the total weight of the steel-braced frame as an objective function, where W_{DL_2} is the weight of the building's dead load after retrofitting, W_{DL_1} is the weight of the building dead load before retrofitting, and W_S is the difference between the two dead loads that give the steel-braced frame weight Equations (2) and (3) define the constraints of lateral displacement of the highest point of the building and inter-story drift, respectively, where d_T is the lateral top displacement, d_T^U is the upper limits of lateral top displacement, d_i is the inter-story drift ratio and is the upper limit of the inter-story ratio stipulated in different codes.

2.3 Optimal Design Procedure

The optimal procedure is performed in two ways; in the first, the distribution of lateral stiffness is inconsistent where there are no constraints in choosing elements cross-section for a certain story concerning upper and lower stories; In contrast, in the second, the stiffness distribution is derived from a consistent distribution form by implicit function to choose the element cross-section. To obtain the optimal solution for the given problem using the Genetic Algorithm, the whole operation, simulated between VB and CSI ETABS, is repeated in cycles until the iterative convergence is reached. Each iteration is a forward step directed to the optimum solution. **Fig. 1** illustrates the optimization procedure carried out between CSI ETABS and VB, while **Fig. 2** shows the flow chart of retrofitting optimization against wind loads.

The steps of the optimization process are listed as follows;

1. Define the design variables, constraints, and the objective function. Identify the limitations of cross-sections based on experiment and experience. Design variables are the cross-sections of steel-braced frame elements. Identify the uppermost limitations for lateral displacement and inter-story drift from the selected code.
2. Build the original CSI ETABS model, define wind loads, and assign the cross-sections to the elements of the braced frame, which are the design variables, with labels defined in the VB code.
3. Set the parameters that control the operation involving the size of the population, the number of crossover and mutation processes, and the size of a new generation.
4. Set the optimization to start and in each iteration, the maximum values of lateral displacement and inter-story drift ratio are obtained.
5. Create the next generation by picking the two chromosomes with the best results within the limitations of defined constraints and making crossover and mutation between them to obtain the next generation.
6. Repeat steps 4 and 5 until the results remain steady, then the optimal solution is obtained.

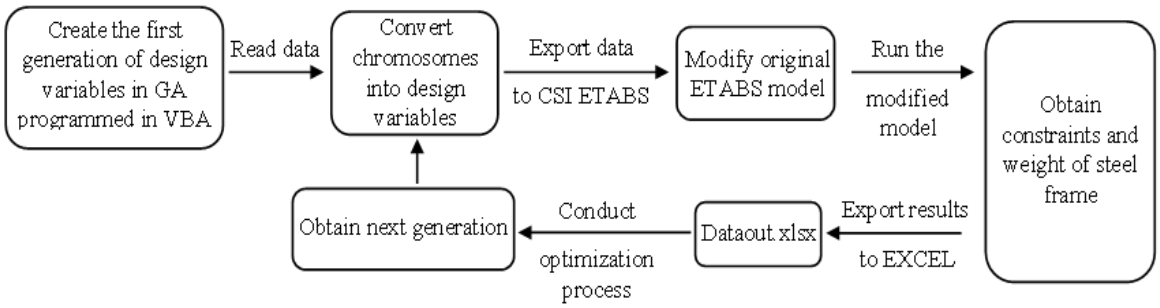

Fig. 1 Flow chart of optimization procedure using VB and CSI ETABS

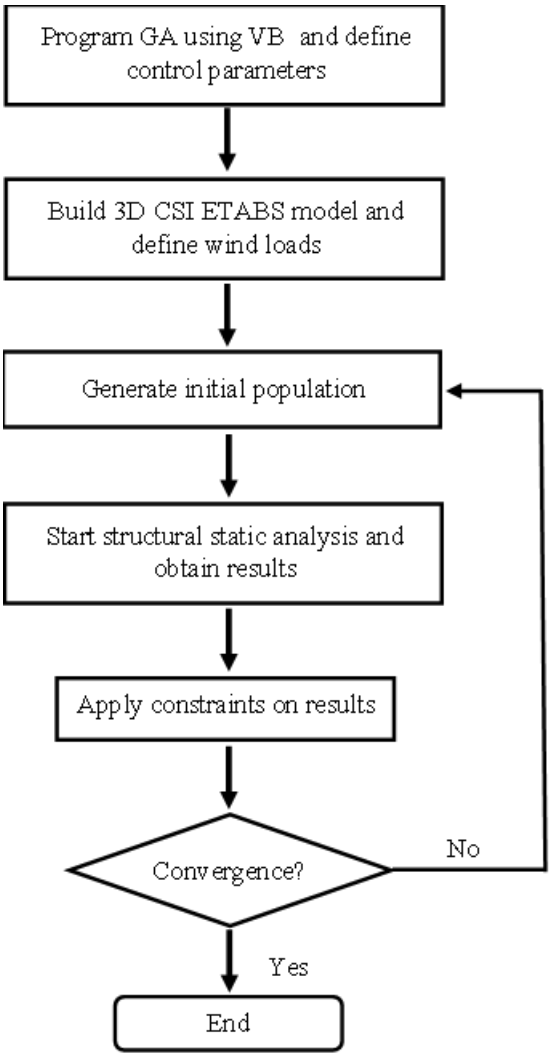

Fig. 2 Flow chart of retrofitting optimization against wind loads

2.4 Graphical User Interface

The implemented software contains two main forms. **Fig. 3** shows the first form that allows the user to select the purpose of the retrofitting system to resist wind or earthquake loads. This form also allows the user to select the design code which determines the uppermost limitations for lateral displacement and inter-story drift. **Fig. 4** shows the second form. In this form, the user selects the prepared original ETABS model file and selects four text files that contain column and bracing labels and the available sections for column and bracing. The stiffness distribution type is selected from the two choices listed before. The maximum number of GA iterations is entered into the software.

After these inputs, the button labeled "Start Optimization" runs the software process. This process may take a few hours or days according to the size of the structure model file. After finishing the optimization process, the implemented software allows the user to display the results, such as the design history to check the stability of the optimization process, optimum sections, and stiffness distribution.

Fig. 3 First form of the Implemented Software

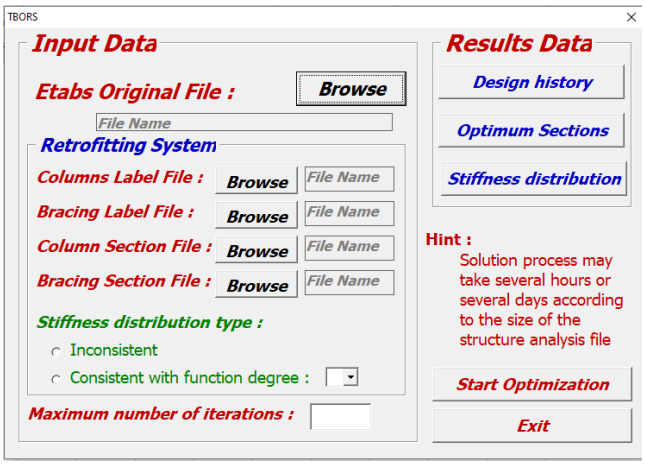

Fig. 4 Second form of the Implemented Software

2.5 Calculation of Equivalent Static Wind Loads (ESWLs)

There are several design codes integrated into the (GUI) to calculate equivalent static wind loads (ESWLs). This paper uses provisions of EN 1991-1-4 (2005)[32] to calculate (ESWLs). The relationship between the mean wind pressure and the mean wind speed, stipulated in EN 1991-1-4 (2005)[32], can be used to determine the mean wind load Fw(z) on a building:

$$F_W = C_s C_d . C_f \left[0.5\, \rho_a\, V_m(Z)^2\right] . A_{ref} \quad (4)$$

where C_s C_d is the structural factor which is normally taken as 1 for framed buildings less than 100 m high; C_f is the force coefficient for the structure which is normally taken as 1.3; ρ_a is the density of air which is normally taken as 1.25 kg/cm^2; $V_m(Z)$ is the mean wind speed at the top of the building; A_{ref} is the reference area.

2.6 Numerical Model

Two rectangular reinforced concrete buildings with dimensions (50 m X 16 m) are used as case models for the optimization problem to obtain the optimum retrofitting system to resist wind loads. The first case is a regular model in terms of the horizontal plan and elevation which faces the wind-induced loads, this case represents the study of wind loads as the impact on regular buildings. The other model is irregular in elevation as it has two different levels, where half of the building is rising to the level of height H which is a variable value and the other half is rising to the level of height 1.5 H. Both two cases are studied 5 times with 5 different heights: 15, 18, 21, 24, and 27 stories. The height of each floor is 3.00 m. The properties of the building materials are listed in **Table 1**. The upstream wind belongs to Terrain category 0 (Sea, coastal area exposed to the open sea) specified in EN 1991-1-4 (2005)[32]. The diaphragm used in the structural modeling and analysis for all floors is rigid. The ESWLs are applied on the geometric center of each floor of the building.

Table 1 Material characteristics

Material	Weight of unit of volume (kN/m^3)	Modulus of elasticity (kN/m^2)	Poisson's ratio
Concrete	25	2 x 10^8	0.2
Steel	78.5	2 x 10^9	0.3

2.7 CSI ETABS Model

As mentioned previously, this paper discusses two different cases that have the same geometric plan but different in elevation the first case is a regular symmetric building as shown in **Fig. 5**, which represents an instance of the studied models that were created on CSI ETABS, while the second case is irregular in elevation as shown in **Fig. 6**, in which there are two levels in the building. The building in the second case is divided into two halves equal in area. The right half is elevated to a height equal to 1.5 the height of the left one. For both cases, external and internal column dimensions are assigned as if they are not designed to resist wind loads. The columns are located every 5 m in the X-direction while they are located every 4 m in the Y-direction, thus each bay is 5 m X 4 m. The thickness of each slab is 150 mm. It is assumed that there is a fixed connection between the building and its foundation. In the regular model, a reinforced concrete core is located in the center of the building with a U shape and dimensions are 4 m in X-direction and 3 m in Y-direction. The thickness of the core wall is 300 mm. Two vertical braced steel frames are erected in the two openings of the architecture plan. Opening dimensions are (4 m X 4 m). Columns of the erected frames are assigned as box sections, whereas bracings are assigned as pipe sections. The building is strengthened by four columns and eight vertical bracings on all floors for each opening. The sectional dimensions' maximum and minimum values of box and pipe sections are specified by engineering experience, avoiding slender sections, while setting the steel sections' dimensions. The cross sections of columns and vertical bracing are considered discrete variables. The list from which GA picks the suitable section for columns and vertical bracings consists of 216 box sections and 120 pipe sections, respectively. The lower and upper sectional dimensions limits of box-sections are BOX (200X200X10) mm and BOX (1500X1500X82) mm, respectively. The lower and upper sectional dimensions limits of pipe sections are PIPE (150X7) mm and PIPE (900X52) mm, respectively. .

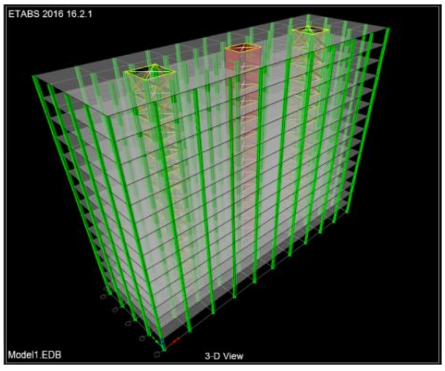

(a) 3-D model

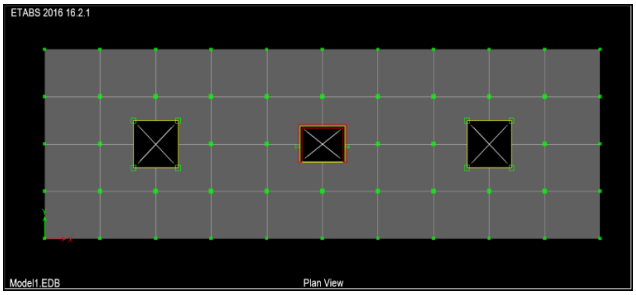

(b) Plan view

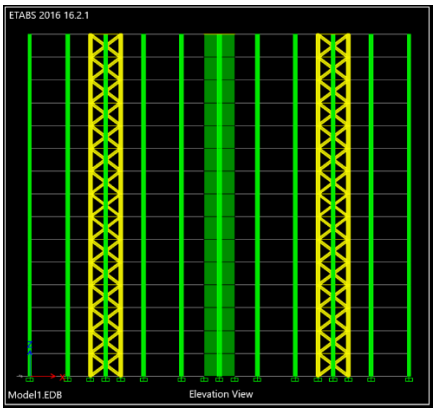

(c) Elevation view

Fig. 5 3-D CSI ETABS 15-story model (Case 1)

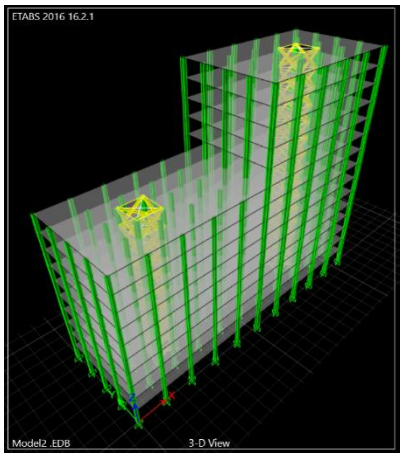

(a) 3-D model

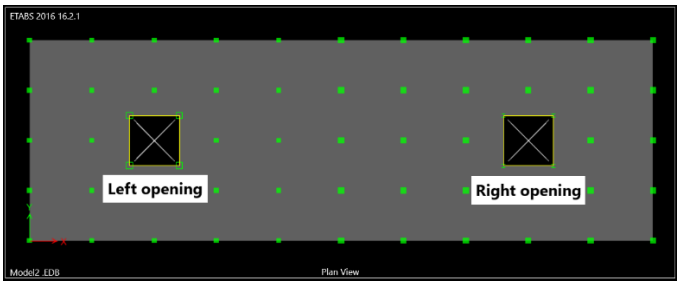

(b) Plan view

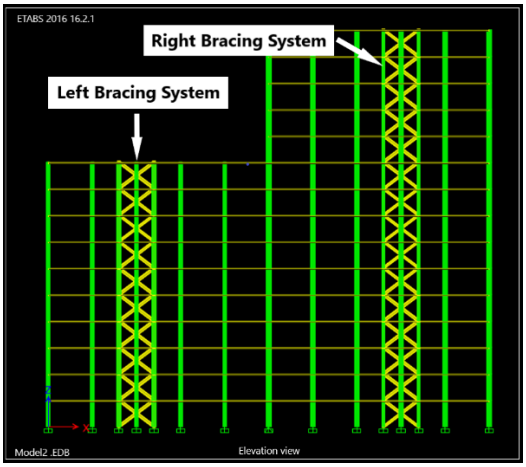

(c) Elevation view

Fig. 6 3-D CSI ETABS 15-story model (Case 2)

2.8 Verification model

Computers and Structures, Inc. (CSI) provides a manual[33] for ETABS2016 software verification which contains example problems used to test various features and capabilities of the ETABS program. By modeling example 3 (Three-Story Plane Frame, Code-Specified Static Lateral Load Analysis), hand-calculated story shears are compared with story shears produced by the ETABS program in **Table 2-1** for UBC seismic loads, **Table 2-2** for ASCE 7-02 seismic loads, and **Table 2-3** for UBC wind loads. The results comparison shows an exact match between the ETABS results and the theoretical data.

Table 2-1 Comparison of Results for Story Shears - UBC 1997 Seismic

Level	ETABS (kips)	Theoretical (kips)	Error (%)
Roof	34.07	34.09	0.06
2nd	56.78	56.82	0.07
1st	68.13	68.19	0.09

Table 2-2 Comparison of Results for Story Shears - ASCE 7-02 Seismic

Level	ETABS (kips)	Theoretical (kips)	Error (%)
Roof	19.37	19.38	0.05
2nd	32.23	32.25	0.06
1st	38.61	38.64	0.08

Table 2-3 Comparison of Results for Story Shears - UBC 1997 Wind

Level	ETABS (kips)	Theoretical (kips)	Error (%)
Roof	3.3	3.3	0.00
2nd	9.49	9.4	0.96
1st	15.21	15.21	0.00

2.9 VB Optimization Model

The optimization process is performed on the CSI ETABS model which is labeled as the original model, while in the coding model, it is imported as M1.EDB. As mentioned before the original model is an RC building that is aimed to be retrofitted and strengthened by a steel-braced frame. First and before the optimization process, the original model is created manually with random steel-braced frame cross-sections. Then, the VB optimization coding opens the CSI ETABS user interface and calls the original model. The objective function and constraints are defined in the VB code. After that, Programmed GA generates a first generation of chromosomes that describes the discrete variables of the optimization model which represent the cross-sections of steel braced frame (columns and vertical bracings). At the same time, the VB code reads the original model selects the steel cross sections on each floor separately and assigns new cross sections to these selected sections according to the first generation that is created randomly. These newly assigned steel cross sections are defined previously and prepared in a list integrated with the VB code. Then, programmed GA determines the objective function (steel weight) and applies the constraints. By applying the penalty function to the population of the first generation, the GA excludes the individuals that don't meet the constraints. After that, GA performs the natural selection and operates mutation and crossover to create the next generation. The whole process is repeated till the GA reaches the optimal model that has minimum weight and meets the constraint.

3. Results and discussion

3.1 Case 1 (Regular Case)

In the beginning, the optimization process took the path in which GA randomly chose the cross-sections of columns and bracings, where there are no constraints in determining the cross-sections of the steel bracing system concerning the adjacent floors, which is labeled "inconsistent stiffness distribution". This case is

performed for two models; 15 and 18-story. The results of these two models are illustrated in **Table 3**,

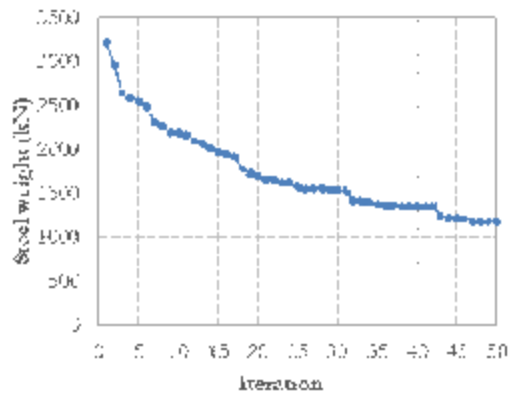

Fig. 1 Optimization history of steel weight of 15-story model (inconsistent)

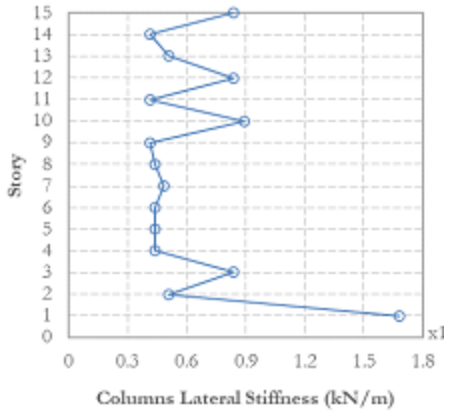

Fig. 2 Stiffness profile of 15-floor model (inconsistent)

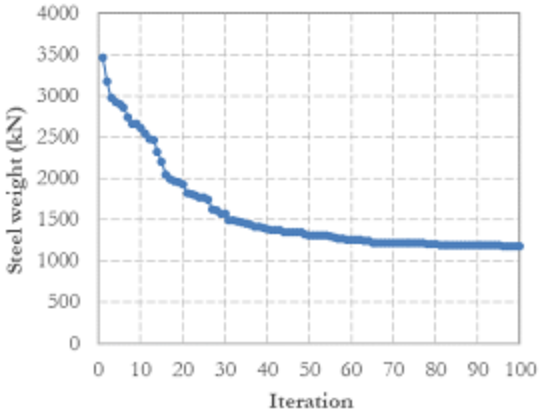

Fig. 3 Optimization history of steel weight of 18-story model (inconsistent)

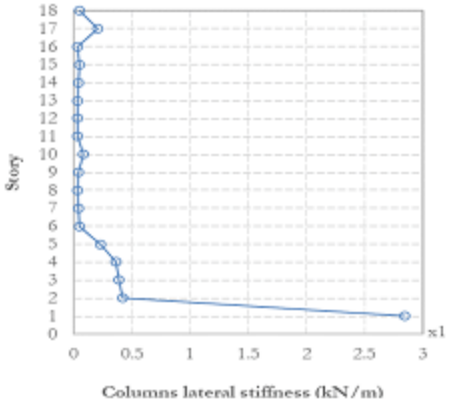

Fig. 4 Stiffness profile of 18-floor model (inconsistent)

Table 4, **Error! Reference source not found.**, **Error! Reference source not found.**, **Error! Reference source not found.**, and, **Error! Reference source not found.**.

Table 3 Cross-sections of columns and bracings for the optimum inconsistent retrofitting system of a 15-story building

Story	Column section	Bracing section	Story	Column section	Bracing section
1st	BOX(300X300X15)	PIPE(250X13)	9th	BOX(200X200X13)	PIPE(200X15)
2nd	BOX(200X200X17)	PIPE(250X12)	10th	BOX(250X250X14)	PIPE(250X13)
3rd	BOX(250X250X13)	PIPE(200X13)	11th	BOX(200X200X13)	PIPE(200X15)
4th	BOX(200X200X14)	PIPE(200X15)	12th	BOX(250X250X13)	PIPE(300X15)
5th	BOX(200X200X14)	PIPE(200X14)	13th	BOX(200X200X17)	PIPE(200X15)
6th	BOX(200X200X14)	PIPE(250X15)	14th	BOX(200X200X13)	PIPE(250X13)
7th	BOX(200X200X16)	PIPE(200X13)	15th	BOX(250X250X13)	PIPE(200X13)
8th	BOX(200X200X14)	PIPE(200X13)			

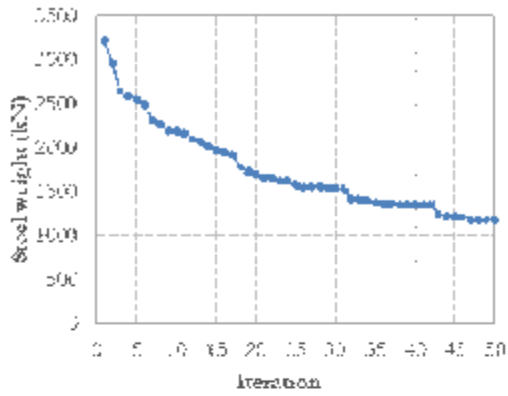

Fig. 1 Optimization history of steel weight of 15-story model (inconsistent)

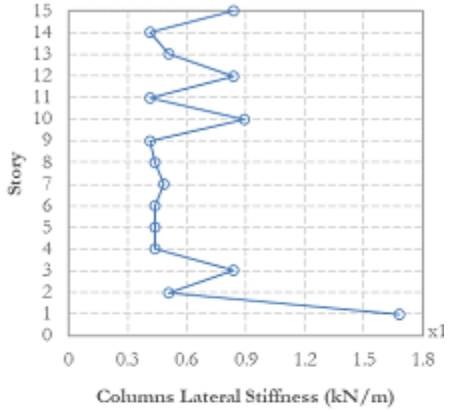

Fig. 2 Stiffness profile of 15-floor model (inconsistent)

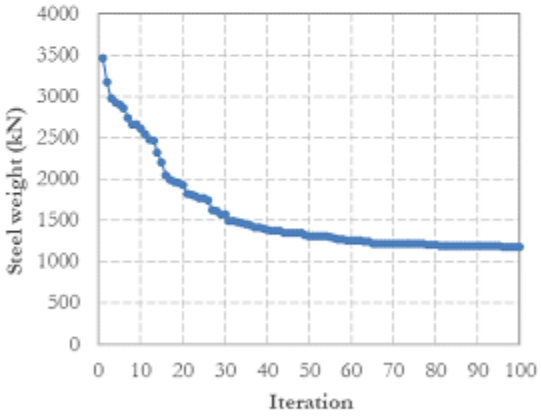

Fig. 3 Optimization history of steel weight of 18-story model (inconsistent)

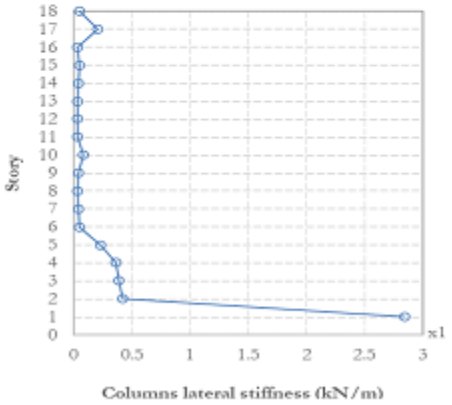

Fig. 4 Stiffness profile of 18-floor model (inconsistent)

Table 4 Cross-sections of columns and bracings for the optimum inconsistent retrofitting system of an 18-story building

Story	Column section	Bracing section	Story	Column section	Bracing section
1st	BOX(600X600X32)	PIPE(150X7)	10th	BOX(250X250X13)	PIPE(150X8)
2nd	BOX(350X350X25)	PIPE(400X20)	11th	BOX(200X200X10)	PIPE(150X7)
3rd	BOX(350X350X23)	PIPE(500X29)	12th	BOX(200X200X10)	PIPE(200X10)
4th	BOX(350X350X21)	PIPE(350X17)	13th	BOX(200X200X10)	PIPE(150X8)
5th	BOX(300X300X22)	PIPE(500X25)	14th	BOX(200X200X12)	PIPE(150X7)
6th	BOX(200X200X15)	PIPE(200X14)	15th	BOX(200X200X15)	PIPE(350X21)
7th	BOX(200X200X14)	PIPE(250X16)	16th	BOX(200X200X11)	PIPE(200X14)
8th	BOX(200X200X11)	PIPE(200X10)	17th	BOX(300X300X19)	PIPE(350X19)
9th	BOX(200X200X13)	PIPE(150X8)	18th	BOX(200X200X17)	PIPE(250X18)

Table 3 and

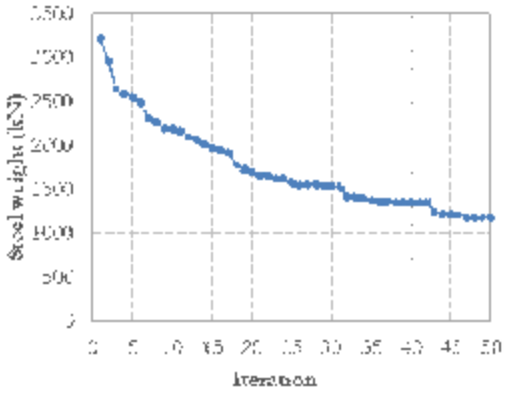

Fig. 1 Optimization history of steel weight of 15-story model (inconsistent)

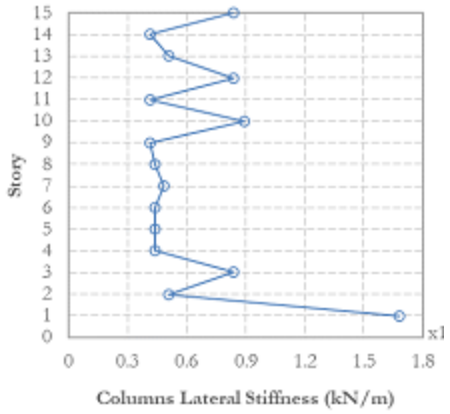

Fig. 2 Stiffness profile of 15-floor model (inconsistent)

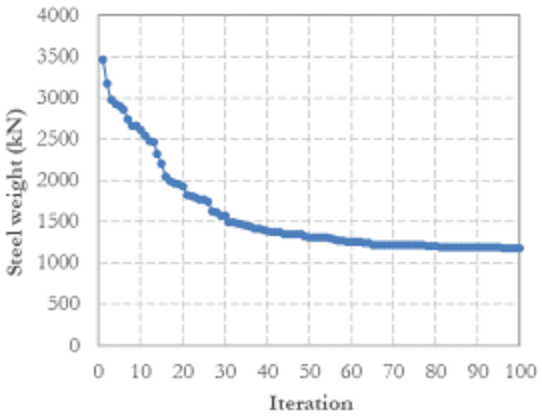

Fig. 3 Optimization history of steel weight of 18-story model (inconsistent)

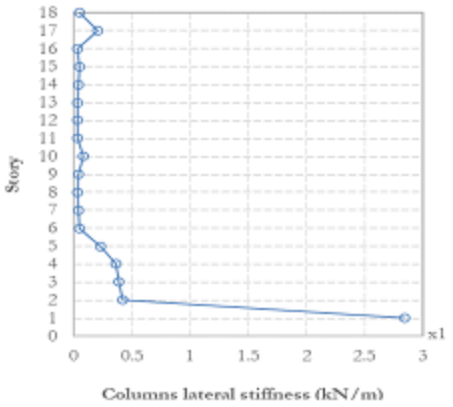

Fig. 4 Stiffness profile of 18-floor model (inconsistent)

Table 4 show the cross-sections of columns and bracings on all floors for 15 and 18-story buildings. The cross-sections are chosen randomly by GA with no constraints to define the correlation between cross-sections of successive floors. **Error! Reference source not found.** and, **Error! Reference source not found.** illustrate optimal design history which indicates the slow speed of the optimization process. To get the lateral stiffness distribution of steel columns with building height, **Error! Reference source not found.** and **Error! Reference source not found.** are used to show this distribution labeled as "stiffness profile". It turns out that the stiffness profile has no pattern which cannot be considered as a general conclusion. Furthermore, it's structurally inaccurate, since there could be a gap and a large variance in the cross-sections between successive floors. Hence, GA was reprogrammed and included constraints to meet the provisions of building codes to keep the lateral stiffness of structural members in successive floors convergent as well as to avoid soft story conditions to have a structurally valid product which is labeled "consistent distribution" and its results are presented in **Table 5**, **Fig. 7** and **Fig. 8**.

Table 5 Cross-sections of columns and bracings for the optimum consistent retrofitting system of a 15-story building

Story	Column section	Bracing section	Story	Column section	Bracing section
1st	BOX(600X600X31)	PIPE(150X7)	9th	BOX(450X450X23)	PIPE(150X7)

2nd	BOX(550X550X35)	PIPE(150X7)	10th	BOX(400X400X21)	PIPE(150X7)
3rd	BOX(550X550X33)	PIPE(150X7)	11th	BOX(350X350X18)	PIPE(150X7)
4th	BOX(550X550X29)	PIPE(150X7)	12th	BOX(250X250X17)	PIPE(150X7)
5th	BOX(500X500X32)	PIPE(150X7)	13 th	BOX(250X250X19)	PIPE(150X7)
6th	BOX(500X500X29)	PIPE(150X7)	14 th	BOX(350X350X18)	PIPE(150X7)
7th	BOX(500X500X25)	PIPE(150X7)	15 th	BOX(400X400X20)	PIPE(150X7)
8th	BOX(450X450X28)	PIPE(150X7)			

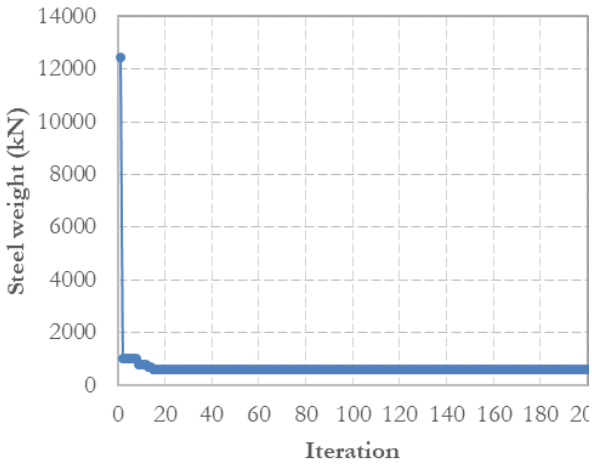

Fig. 7 Optimization history of steel weight of 15-floor model (consistent)

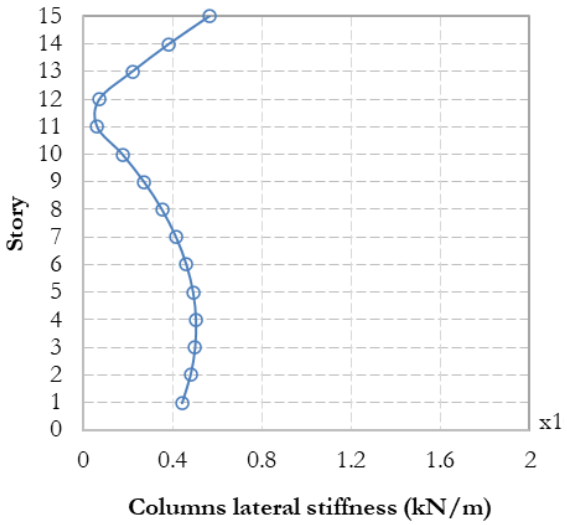

Fig. 8 Stiffness profile of 15-floor model (consistent)

In **Fig. 7**, it is evident that the variation of steel weight with the iteration cycles remains with the same pattern and remains constant from an early stage of the optimization process till its end at the 200th iteration, which means the GA in this model has found the optimal profile of lateral stiffness from the beginning. Therefore, there was no need to keep conducting the optimization process. From **Fig. 8**, which shows the stiffness profile of a 15-story model for consistent distribution, the lateral stiffness of columns has a maximum value of 4.4 x10^4 kN/m on the first floor to increase the overall lateral stiffness of the building, which is meaningful to begin from its base. Then, the lateral stiffness decreases gradually to reach the minimum value of 5.98 x10^3 kN/m at the 11th floor, which assures the concept of the cantilever action, as the lower floors are subjected to much larger moments and shear forces than the upper ones, after that it increases again at 15th floor. This inflection in lateral stiffness in upper floors works to disperse the wind-induced force. **Fig. 7** shows the optimal design history which indicates the rapid speed of the optimization process.

Likewise, the stiffness profile of the 18-story model is shown in **Fig. 9**, where the lateral stiffness of columns has a maximum value of 7.26 x 10^5 kN/m on the first floor. Then, the lateral stiffness decreases gradually to reach a minimum value of 1x10^4 kN/m on the 14th floor. After that, it increases again at the upper floors till the 18th floor.

Fig. 10, **Fig. 11**, and, **Fig. 12** present the stiffness profile of the same case plan of heights 21-story, 24-story, and 27-story, respectively. The other plotted stiffness profiles assure the trend of cantilever action, where the maximum values of lateral stiffness are at the first floors which are 6.8 x10^6 kN/m, 3.65 x10^7 kN/m, and 1.12 x10^7 kN/m, respectively, while the minimum values are 9.34 x10^4 kN/m, 1.14 x10^5 kN/m and 3.49 x10^5 kN/m, respectively.

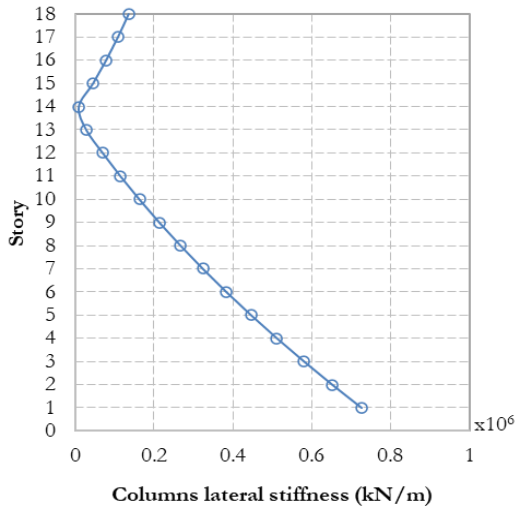

Fig. 9 Stiffness profile of 18-floor model (consistent)

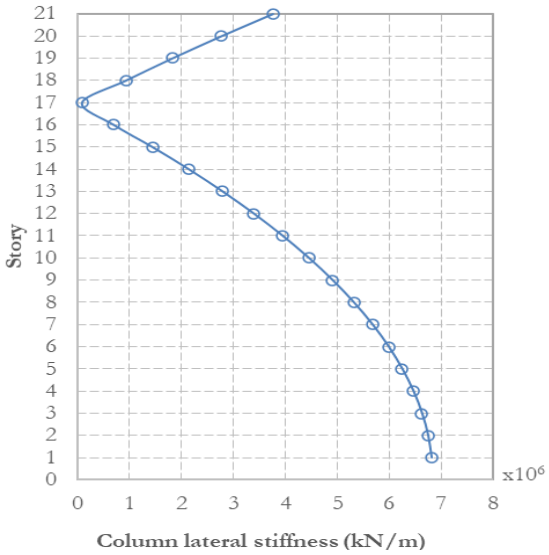

Fig. 10 Stiffness profile of 21-floor model (consistent)

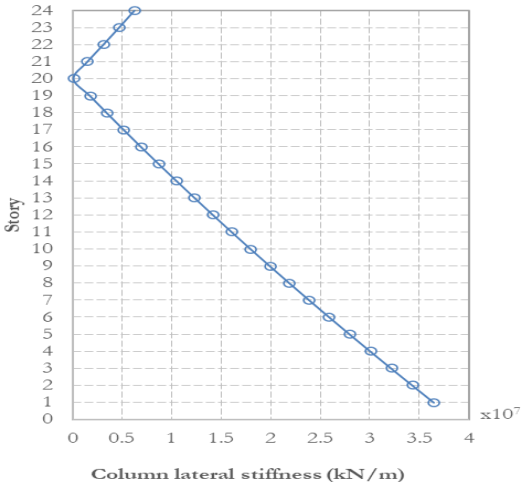

Fig. 11 Stiffness profile of 24-floor model (consistent)

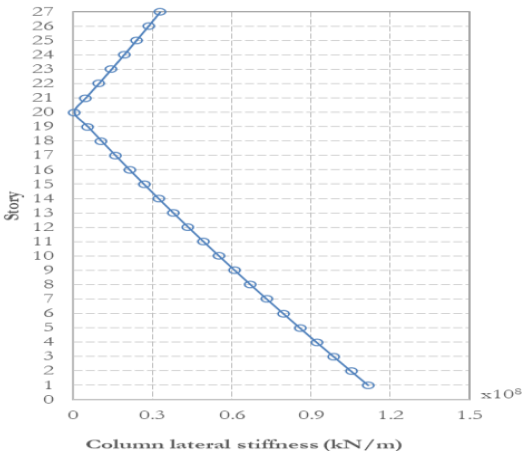

Fig. 12 Stiffness profile of 27-floor model (consistent)

For each case, the ratio of the minimum lateral-stiffness point height from the base (h) to the total building height (H) is presented in **Fig. 13**, which shows that, as the building height increases the ratio slightly increases then decreases at the 27-story model. The relation between the ratio (h/H) and total building height (H) is presented by the following equation:

$$f(H) = -7 \times 10^{-7} H^4 + 2 \times 10^{-4} H^3 - 1.4 \times 10^{-2} H^2 + 0.5808 H - 7.87 \quad (5)$$

where f(H) is the ratio (h/H)

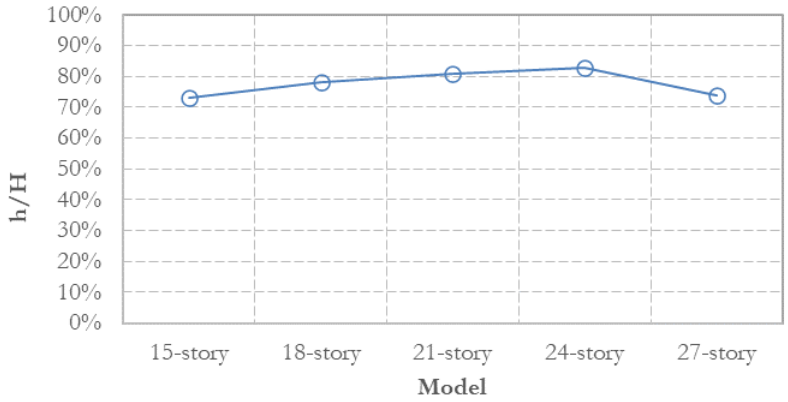

Fig. 13 Ratio of the height of minimum floor stiffness to the total height vs. Model

It is observed from the stiffness profiles that, as the building height increases, the GA chooses larger initial stiffness values at the first floor of each case, where the values of initial stiffness values are 4.4 x10^4 kN/m, 7.26 x 10^5, 6.8 x10^6 kN/m, 3.65 x10^7 kN/m, and 1.12 x10^7 kN/m, respectively. These results are presented to the building height in **Fig. 14**, which illustrates the upward curve of the initial stiffness as the building height is increased. By interpolation, the following equation, describing the initial stiffness of the steel braced frame as a function of total building height, can be deduced:

$$k(H)= 24.015\ H^4 - 1460.6\ H^3 - 1.52 \times 10^5\ H^2 + 1 \times 10^7\ H - 3 \times 10^8 \quad (6)$$

where k(H) is the initial stiffness of the steel braced frame and H is the total building height above the ground.

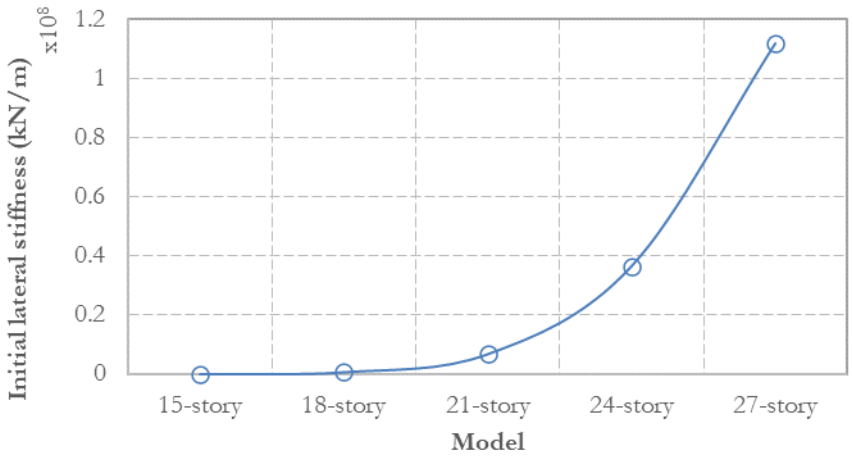

Fig. 14 Initial lateral stiffness vs. Model

Besides, as the building height increases, the decreasing rate of the stiffness profile (from the first floor to the minimum point) increases. The values of decreasing rates corresponding to heights are shown in **Fig. 15**. This upward curve means that the difference in steel bracing system columns cross-sections between adjacent floors gets larger in higher cases. Hence, the column cross-section profile (which represents the columns' cross-sections corresponding to each floor) is more tapered in higher cases.

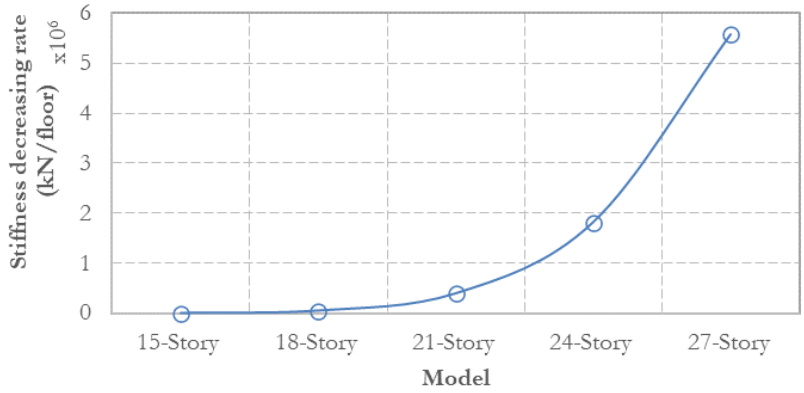

Fig. 15 Stiffness decreasing rate vs. Model

3.2 Case 2 (Irregular Case)

This case study delves into a comprehensive investigation of the profound impacts of wind loads on tall buildings characterized by irregularities. The focal point of the study is a specific building featuring two distinct elevation levels, vividly depicted in **Fig. 6**. This architectural configuration induces an intriguing asymmetry in the distribution of wind pressure across the building facade. Wind loads, traditionally assumed to be uniform, exert their force on the exposed building areas susceptible to wind gusts. In the context of the critical loading scenario, the wind loading is hypothesized to act perpendicular to the building facade. An intriguing aspect of this architectural design is the unequal proportions between the right and left halves of the building. The right half, towering at 1.5 times the height of the left half, shares an equivalent width with its counterpart. This intentional dissimilarity results in the loaded area of the right half being 1.5 times larger than that of the left half. Consequently, the wind force experienced by the right part of the building is also amplified, being 1.5 times greater than the force exerted on the left side. This disparity in forces leads to the manifestation of torsional loading within the building structure, unraveling additional layers of complexity in the dynamic interaction between wind and architecture.

Figs. 20 to **24** display the stiffness profiles of steel columns for both left and right bracing systems for each model. The initial stiffness of the columns of the left bracing system of the 15-story model is depicted as 1.38×10^5 kN/m, whereas the columns of the right bracing system exhibit an initial value of 4.8×10^4 kN/m, as shown in Fig. 16. Similarly, **Figs. 21, 22, 23, and 24** reveal that the 18-story, 21-story, 24-story, and 27-story models have values of column stiffness of the left bracing system of 3.3×10^6 kN/m, 5.6×10^6 kN/m, 2.7×10^7 kN/m, and 4.7×10^7 kN/m, respectively. The corresponding initial stiffness values for the right bracing systems in these models are 2.3×10^5 kN/m, 5.6×10^6 kN/m, 9.5×10^6 kN/m, and 2.3×10^5 kN/m, respectively. The figures displaying the stiffness profile curves consistently confirm the pattern established in the initial scenario, where the stiffness profile consistently commences at the first floor with the cross-section featuring the highest lateral stiffness value across the entire profile. Subsequently, the stiffness profile gradually decreases to a certain point in profile height, with this point varying among models based on the profile's height and initial value on the first floor. Following this descent, as depicted in the figures, the stiffness profile undergoes an upward trend, designating the inflection point as the boundary that separates the building into two sections. This inflection point effectively absorbs a portion of the shear force applied to the upper section, leading to a reduction in the cumulative impact of stronger wind loads on lower floors. Consequently, the lower floors necessitate relatively smaller cross-sections compared to scenarios where the stiffness profile initiates with the highest value on the first floor and concludes with the lowest value on the last floor. When comparing the stiffness profiles between the left and right bracing systems across various models (15-story, 18-story, 21-story, 24-story, and 27-story), a consistent observation is made: the left bracing system consistently exhibits either larger or equal stiffness profiles (larger cross sections) in comparison to the right bracing system. This is noteworthy, given that the right half of the building is subjected to greater wind loads due to its larger exposure area to wind gusts. However, the left bracing system maintains larger cross sections. This phenomenon can be elucidated by recognizing the inverse relationship between stiffness

and height; as the building height increases, it becomes more slender. If the right bracing system were to possess a larger stiffness profile instead of the left one, the overall lateral stiffness of the building would be diminished compared to the scenario where the left bracing system dominates in stiffness profile size. Given that the objective function pertains to the total weight of stiffening steel, it is structurally and economically optimal to assign the larger stiffness profile to the left bracing system rather than the right one, aiming to achieve the highest overall lateral stiffness value with the minimum weight of stiffening steel possible.

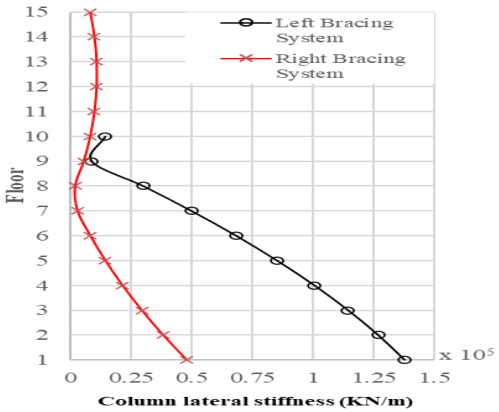

Fig. 16 Stiffness profile of 15-floor model (Case 2)

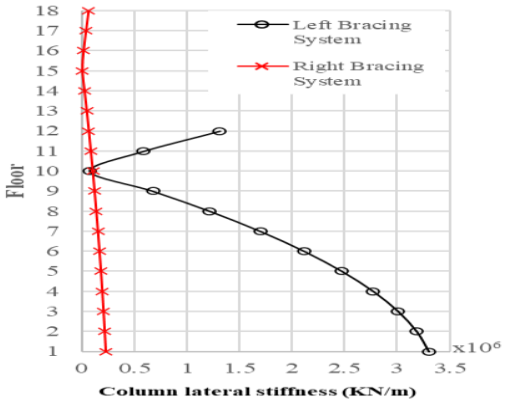

Fig. 17 Stiffness profile of 18-floor model (Case 2)

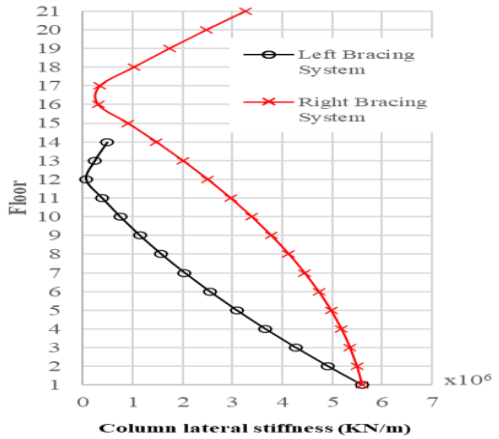

Fig. 18 Stiffness profile of 21-floor model (Case 2)

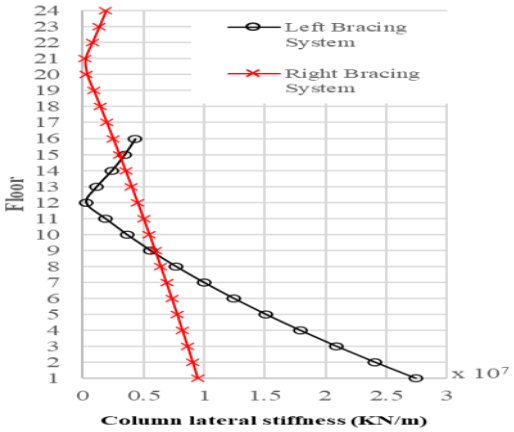

Fig. 19 Stiffness profile of 24-floor model (Case 2)

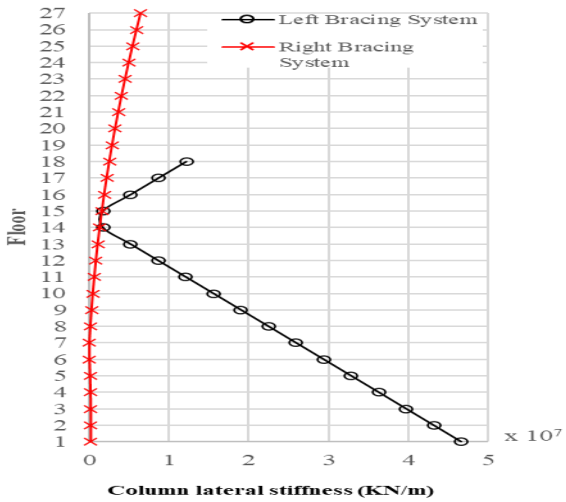

Fig. 20 Stiffness profile of 27-floor model (Case 2)

4. Conclusion

This paper proposes a retrofitting optimization technique for a vulnerable building against wind loads using steel-braced frames in the openings of the building's architectural plan. The optimal weight of strengthening structural steel members represented in the form of an optimal lateral stiffness distribution of steel columns with building height is obtained using an effective optimization method presented by programmed simulation between VB and CSI ETABS in which Genetic algorithm (GA) is involved as an optimization algorithm. An optimal lateral stiffness distribution of steel columns has been obtained from the results of several optimization iterations on various heights of the case study building model. All of these distributions have the same conceptual form in which the stiffness value of columns in the lower stories columns is the greatest. Then, the stiffness value regularly decreases till reaching the middle of the final third of the building height after that the stiffness increases till the last story. This form of lateral stiffness distribution makes the building able to fulfill the constraints of responses induced by wind involving top displacements and inter-story drift ratios. The results show that the proposed technique makes the building effectively capable of resisting wind excitations in terms of structural safety and serviceability.

Statements and Declarations

Competing Interest

The authors declare that they have no known competing financial interests or personal relationships that could have appeared to influence the work reported in this paper.

Credit Authorship

Rania Samir: Conceptualization, Formal analysis, Methodology, Project administration, Supervision,

, Software, Writing – review.

Mohamed Abdel-Hamed: Conceptualization, Data curation, Visualization, Resources, Investigation, Writing-original draft.

Atef Eraky: Conceptualization, Formal analysis, Methodology, Project administration, Supervision, Software, Writing – review.

Abdallah Salama: Conceptualization, Methodology, Supervision, Writing- review.

Data Availability

Data will be made available on request

References

[1] T. F. A. de Lavôr, J. L. V. de Brito, and A. M. Loredo-Souza, “Interference effects mapping on the static wind loading of a tall building,” *Lat. Am. J. Solids Struct.*, vol. 20, no. 3, pp. 1–17, 2023, doi: 10.1590/1679-78257330.

[2] F. M. B. Parfitt, I. B. Morsch, and H. M. Gomes, “Multi-objective optimization of outriggers in high-rise buildings subjected to wind loads,” *Rev. IBRACON Estruturas e Mater.*, vol. 16, no. 2, pp. 1–19, 2023, doi: 10.1590/s1983-41952023000200003.

[3] F. Alkhatib, N. Kasim, S. Qaidi, H. M. Najm, and M. M. Sabri Sabri, “Wind-resistant structural optimization of irregular tall building using CFD and improved genetic algorithm for sustainable and cost-effective design,” *Front. Energy Res.*, vol. 10, no. October, 2022, doi: 10.3389/fenrg.2022.1017813.

[4] M. Halis Gunel and H. Emre Ilgin, “A proposal for the classification of structural systems of tall buildings,” *Build. Environ.*, vol. 42, no. 7, pp. 2667–2675, 2007, doi: 10.1016/j.buildenv.2006.07.007.

[5] A. Elshaer, A. Gairola, K. Adamek, and G. Bitsuamlak, “Variations in wind load on tall buildings due to urban development,” *Sustain. Cities Soc.*, vol. 34, pp. 264–277, 2017, doi: 10.1016/j.scs.2017.06.008.

[6] F. Hou and M. Jafari, "Investigation approaches to quantify wind-induced load and response of tall buildings: A review," *Sustain. Cities Soc.*, vol. 62, no. September 2019, p. 102376, 2020, doi: 10.1016/j.scs.2020.102376.

[7] Y. M. Kim and K. P. You, "Dynamic responses of a tapered tall building to wind loads," *J. Wind Eng. Ind. Aerodyn.*, vol. 90, no. 12–15, pp. 1771–1782, 2002, doi: 10.1016/S0167-6105(02)00286-6.

[8] A. Sharma, H. Mittal, and A. Gairola, "Mitigation of wind load on tall buildings through aerodynamic modifications: Review," *J. Build. Eng.*, vol. 18, no. September 2017, pp. 180–194, 2018, doi: 10.1016/j.jobe.2018.03.005.

[9] M. Gu and Y. Quan, "Across-wind loads of typical tall buildings," *J. Wind Eng. Ind. Aerodyn.*, vol. 92, no. 13, pp. 1147–1165, 2004, doi: 10.1016/j.jweia.2004.06.004.

[10] D. K. Kwon and A. Kareem, "Comparative study of major international wind codes and standards for wind effects on tall buildings," *Eng. Struct.*, vol. 51, pp. 23–35, 2013, doi: 10.1016/j.engstruct.2013.01.008.

[11] J. N. Yang, S. L. Lin, J. H. Kim, and A. K. Agrawal, "Optimal design of passive supplemental dampers based on H∞ and H 2 performances," *Struct. Congr. 2000 Adv. Technol. Struct. Eng.*, vol. 103, pp. 1–8, 2004, doi: 10.1061/40492(2000)8.

[12] Y. Li, R. B. Duan, Q. S. Li, Y. G. Li, and X. Huang, "Wind-resistant optimal design of tall buildings based on improved genetic algorithm," *Structures*, vol. 27, no. August, pp. 2182–2191, 2020, doi: 10.1016/j.istruc.2020.08.036.

[13] Q. S. Li, X. K. Zou, J. R. Wu, and Q. Wang, "Integrated wind-induced response analysis and design optimization of tall steel buildings using Micro-GA," *Struct. Des. Tall Spec. Build.*, vol. 20, pp. 951–971, 2011.

[14] J. W. Zhang and Q. S. Li, "Mitigation of wind-induced vibration of a 600 m high skyscraper," *Int. J. Struct. Stab. Dyn.*, vol. 19, no. 2, 2019, doi: 10.1142/S0219455419500159.

[15] Q. S. Li, L.-H. Zhi, A. Y. Tuan, C.-S. Kao, S.-C. Su, and C.-F. Wu, "Dynamic Behavior of Taipei 101 Tower: Field Measurement and Numerical Analysis," *J. Struct. Eng.*, vol. 137, no. 1, pp. 143–155, Jun. 2010, doi: 10.1061/(ASCE)ST.1943-541X.0000264.

[16] A. Miano, H. Sezen, F. Jalayer, and A. Prota, "Performance-based comparison of different retrofit methods for reinforced concrete sructures," *COMPDYN 2017 - Proc. 6th Int. Conf. Comput. Methods Struct. Dyn. Earthq. Eng.*, vol. 1, no. June, pp. 1515–1535, 2017, doi: 10.7712/120117.5510.17150.

[17] B. L. Karihoo, F. J. Alaee, and S. D. P. Benson, "A new technique for retrofitting damaged concrete structures," *Proc. Inst. Civ. Eng. Struct. Build.*, vol. 152, no. 4, pp. 309–318, 2002, doi: 10.1680/stbu.152.4.309.40812.

[18] A. B. M. Rafiqul Haque and M. Shahria Alam, "Optimal retrofitting method selection for RC frame structures: A case study," *Proceedings, Annu. Conf. - Can. Soc. Civ. Eng.*, vol. 3, no. Mcdm, pp. 1974–1982, 2012.

[19] D. K. Kim and J. W. Hu, "Bracing systems for seismic and wind performance of tall buildings," *Adv. Mater. Res.*, vol. 650, pp. 667–672, 2013, doi: 10.4028/www.scientific.net/AMR.650.667.

[20] A. Vafai, H. Estekanchi, and M. Mofid, "The use of single diagonal bracing in improvement of the lateral response of tall buildings," *Struct. Des. Tall Build.*, vol. 4, no. 2, pp. 115–126, 1995, doi: 10.1002/tal.4320040203.

[21] C. M. Foley, M. Asce, S. Pezeshk, M. Asce, A. Alimoradi, and A. M. Asce, "Probabilistic Performance-Based Optimal Design of Steel Moment-Resisting Frames . I : Formulation," no. June, 2007.

[22] C. M. Chan and X. K. Zou, "Elastic and inelastic drift performance optimization for reinforced concrete buildings under earthquake loads," *Earthq. Eng. Struct. Dyn.*, vol. 33, no. 8, pp. 929–950, 2004, doi: 10.1002/eqe.385.

[23] C.-M. Chan and Q. Wang, "Nonlinear Stiffness Design Optimization of Tall Reinforced Concrete Buildings under Service Loads," *J. Struct. Eng.*, vol. 132, no. 6, pp. 978–990, 2006, doi: 10.1061/(asce)0733-9445(2006)132:6(978).

[24] C. M. Chan, J. K. L. Chui, and M. R. Huang, "Integrated aerodynamic load determination and stiffness design optimization of tall buildings," *Struct. Des. Tall Spec. Build.*, vol. 18, no. 1, pp. 59–80, 2009, doi:

10.1002/tal.397.

[25] M. F. Huang, C. M. Chan, and W. J. Lou, "Optimal performance-based design of wind sensitive tall buildings considering uncertainties," *Comput. Struct.*, vol. 98–99, pp. 7–16, 2012, doi: 10.1016/j.compstruc.2012.01.012.

[26] Y. Li and Q. S. Li, "Wind-induced response based optimal design of irregular shaped tall buildings," *J. Wind Eng. Ind. Aerodyn.*, vol. 155, pp. 197–207, 2016, doi: 10.1016/j.jweia.2016.06.001.

[27] A. Xu, W. X. Sun, R. H. Zhao, J. R. Wu, and W. Q. Ying, "Lateral drift constrained structural optimization of an actual supertall building acted by wind load," *Struct. Des. Tall Spec. Build.*, vol. 26, no. 6, pp. 1–13, 2017, doi: 10.1002/tal.1344.

[28] J. Y. Fu, B. G. Wu, A. Xu, J. R. Wu, and Y. L. Pi, "A new method for frequency constrained structural optimization of tall buildings under wind loads," *Struct. Des. Tall Spec. Build.*, vol. 27, no. 18, 2018, doi: 10.1002/tal.1549.

[29] S. Gholizadeh and F. Fattahi, "Design optimization of tall steel buildings by a modified particleswarm algorithm," *Struct. Des. Tall Spec. Build.*, vol. 23, pp. 285–301, 2014, doi: 10.1002/tal.1042.

[30] C. M. Chan and P. Liu, "Design optimization of practical tall concrete buildings using hybrid optimality criteria and genetic algorithms," *Proc. 8th Int. Conf. Comput. Civ. Build. Eng.*, vol. 279, pp. 263–270, 2000, doi: 10.1061/40513(279)34.

[31] H. Lu and X. Guo, "Optimization of reinforced concrete tall buildings using a hybrid genetic algorithm," *Appl. Mech. Mater.*, vol. 94–96, pp. 815–819, 2011, doi: 10.4028/www.scientific.net/AMM.94-96.815.

[32] *EN 1991-1-4 (2005) (English): Eurocode 1: Actions on structures - Part 1-4: General actions - Wind actions, The European Union Per Regulation 305/2011, Directive 98/34/EC, Directive 2004/18/EC.*, no. 2005.

[33] I. Computers & Structures, *Software Verification Examples*. 2017. [Online]. Available: http://www.csiamerica.com/